Carbohydrate Polymers 233 (2020) 115844

Contents lists available at ScienceDirect

Carbohydrate Polymers

journal homepage: www.elsevier.com/locate/carbpol

NMR characterization and anticoagulant activity of the oligosaccharides from the fucosylated glycosaminoglycan isolated from *Holothuria coluber*

Wenjiao Yang[a,1], Dingyuan Chen[a,c,1], Zhicheng He[a,c], Lutan Zhou[a,c], Ying Cai[a,c], Hui Mao[a,c], Na Gao[b,*], Zhili Zuo[a,*], Ronghua Yin[a,*], Jinhua Zhao[a,b,d]

[a] State Key Laboratory of Phytochemistry and Plant Resources in West China, Kunming Institute of Botany, Chinese Academy of Sciences, Kunming 650201, China
[b] School of Pharmaceutical Sciences, South-Central University for Nationalities, Wuhan 430074, China
[c] University of Chinese Academy of Sciences, Beijing 100049, China
[d] Guangxi Institute of Traditional Medical and Pharmaceutical Sciences, Nanning 530022, China

ARTICLE INFO

Keywords:
Fucosylated glycosaminoglycan
Oligosaccharide
β-Eliminative depolymerization
Chemical structure
iXase

ABSTRACT

A glycosaminoglycan was isolated from the sea cucumber *Holothuria coluber* (HcFG). A series of oligosaccharide fragments (dp range 3–11) were prepared from its *β*-eliminative depolymerized product (dHcFG). Extensive NMR characterization of the oligosaccharides indicated the D-GlcA-*β*1,3-D-GalNAc$_{4S6S}$ repeating disaccharide backbone was substituted by monosaccharide branches comprising of Fuc$_{2S4S}$, Fuc$_{3S4S}$ and Fuc$_{4S}$, linked to O-3 of D-GlcA. For the prevailing Fuc$_{3S4S}$ at nonreducing end of dHcFG, the *β*-eliminative depolymerization process of HcFG was compared with those of the FGs from *Actinopyga miliaris* (AmFG, branched with Fuc$_{3S4S}$) and *Stichopus variegatus* (SvFG, branched with Fuc$_{2S4S}$). The result suggested that D-GlcA substituted with Fuc$_{3S4S}$ was more susceptible to depolymerization than that with Fuc$_{2S4S}$. It might be due to the larger steric hindrance effects from Fuc$_{2S4S}$ on the esterification of GlcA. Biological assays confirmed that the minimum chain length (dp8), regardless of the Fuc branch types, was required for the potent anti-iXase and anticoagulant activities in FG fragments.

1. Introduction

Sea cucumber with high edible and medicinal value is rich in acid polysaccharides (Bordbar, Anwar, & Saari, 2011). Fucosylated glycosaminoglycan (FG) is one of the most common acid polysaccharides in the body wall of sea cucumber (Myron, Siddiquee, & Al Azad, 2014). Literature reported that FG has a variety of pharmacological activities, such as anti-tumor, anti-inflammation and antithrombosis (Borsig et al., 2007; Mou, Li, Qi, & Yang, 2018; Wu et al., 2015). Particularly, FG has potent anticoagulant activity by inhibiting the intrinsic factor tenase (iXase) in the coagulation cascade (Kitazato, Kitazato, Nagase, & Minamiguchi, 1996; Sheehan & Walke, 2006; Wu et al., 2015).

FG from sea cucumber has three types of monosaccharides, D-glucuronic acid (GlcA), *N*-acetyl-D-galactosamine (GalNAc) and L-fucose (Fuc) (Pomin, 2014). It is generally considered that the backbone of FG consists of alternate D-GlcA and D-GalNAc through β1,3 and β1,4 glycoside bonds, and sulfated fucoses (FucS) are attached to the backbone as branches (Myron et al., 2014; Pomin, 2014; Ustyuzhanina, Bilan, Nifantiev, & Usov, 2019). Nevertheless, the linkage position such as O-3 of GlcA or O-4/6 of GalNAc (Ustyuzhanina et al., 2016; Yoshida & Minami, 1992) and chain length (mono-, di- or tri-fucosyls) (Kariya, Watabe, Hashimoto, & Yoshida, 1990; Kariya, Watabe, Kyogashima, Ishihara, & Ishii, 1997; Vieira & Mourão, 1988; Vieira, Mulloy, & Mourão, 1991; Yang, Wang, Jiang, & Lv, 2015) of FucS branches are yet

Abbreviations: FG, fucosylated glycosaminoglycan; iXase, intrinsic factor tenase; GlcA, D-glucuronic acid; GalNAc, *N*-acetyl-D-galactosamine; Fuc, L-fucose; FucS, sulfated fucose; Fuc$_{2S4S}$, 2,4-di-*O*-sulfated fucose; Fuc$_{3S4S}$, 3,4-di-*O*-sulfated fucose; Fuc$_{4S}$, 4-mono-*O*-sulfated fucose; Fuc$_{3S}$, 3-mono-*O*-sulfated fucose; HcFG, FG from *Holothuria coluber*; SvFG, FG from *Stichopus variegatus*; AmFG, FG from *Actinopyga miliaris*; dHcFG, depolymerized HcFG; dSvFG, depolymerized SvFG; dAmFG, depolymerized AmFG; dp, degree of polymerization; NMR, nuclear magnetic resonance; APTT, activated partial thromboplastin time; PT, prothrombin time; TT, thrombin time; GPC, gel permeation chromatography; HPGPC, high-performance gel permeation chromatography; RID, differential refractive index detector; DAD, diode array detector; IR, infrared spectrum; Mn, number-average molecular weight; Mw, weight-average molecular weight; LMWH, low molecular weight heparin; AT, antithrombin

* Corresponding authors.
E-mail addresses: gn2008.happy@163.com (N. Gao), zuozhili@mail.kib.ac.cn (Z. Zuo), yinronghua@mail.kib.ac.cn (R. Yin).
[1] The authors contributed equally.

https://doi.org/10.1016/j.carbpol.2020.115844
Received 8 November 2019; Received in revised form 7 January 2020; Accepted 7 January 2020
Available online 11 January 2020
0144-8617/

to be ascertained.

Precise structural elucidation of the native FG is challenging because of its large molecular weight and the overlapped 1D NMR spectroscopic signals (Santos, Porto, Soares, Vilanova, & Mourão, 2017). Studies have shown that purified fragments with well-defined structures from depolymerized FG could be applied to reassemble the precise structure of native FG (Santos et al., 2017; Zhao et al., 2015). For purpose of this "bottom up" strategy, *β*-eliminative and deaminative depolymerization methods which could selectively cleave the glycoside bonds D-GalNAc-β1,4-D-GlcA in backbone have been established (Gao et al., 2015; Zhao et al., 2013). In addition, the unambiguous structures of FGs from several sea cucumbers have been reliably clarified by analyzing the structures of fragments purified from depolymerized FGs (Cai et al., 2019; Guan et al., 2019; Shang et al., 2018; Yin et al., 2018; Zhao et al., 2015).

Earlier studies have also shown that native FG displayed potent iXase inhibitory activity with undesired side effects such as factor XII activation and platelet aggregation (Fonseca, Santos, & Mourão, 2009; Li & Lian, 1988). Depolymerization was demonstrated to be a useful approach to reduce such side effects while retaining the potent iXase inhibitory activity (Wu et al., 2015). Hence, the fragments from depolymerized FG could be favorable not only for the structural elucidation, but also for the structure and anticoagulant activity relationship analysis (Cai et al., 2019; Yan et al., 2017; Yin et al., 2018; Zhao et al., 2015).

Indeed, the respective structures of FGs vary in species though they are considered to share a common skeleton (Cai et al., 2019). In our previous work on FG from sea cucumber *Holothuria coluber* (HcFG), we preliminarily elucidated its physicochemical properties and the structure of its oxidative depolymerized product. Therein, several types of FucS (Fuc_{2S4S}, Fuc_{3S4S}, Fuc_{4S} and Fuc_{3S}) were reported (Yang et al., 2018). However, the precise structure and novel structural characteristics in HcFG are yet to be identified. In this work, its depolymerized product (dHcFG) was prepared by *β*-eliminative cleavage, and from which, four oligosaccharide fractions, i.e. tri-, penta-, octa- and hendeca-saccharide were purified. Their structures were determined by NMR spectroscopy. The spectral data recorded indicated that the fucosyl side-chains were all O-3 linked to the *D*-GlcA of the backbone.

Interestingly, according to the integral ratios of the anomeric proton signals from different types of FucS, those found at the nonreducing and reducing end of the oligosaccharides were not equal in mole and were unequal to that of the native HcFG. This phenomenon was observed in the ^{1}H NMR spectra of penta-, octa- and hendeca-saccharide, implying that the glycosidic bonds of β1,4-D-GlcA branched with different types of FucS have different susceptibility to the *β*-elimination reaction.

To verify this hypothesis, the *β*-eliminative reaction was performed on other two FGs, AmFG (branched with Fuc_{3S4S}) and SvFG (branched with Fuc_{2S4S}) (Cai et al., 2019), and the results were compared with that from HcFG. Furthermore, the anticoagulant and anti-iXase activities of the three native FGs with different FucS branches and their corresponding depolymerized products were assessed.

2. Materials and methods

2.1. Materials

Dried body wall of sea cucumber *H. coluber* was purchased from seafood markets in Guangzhou city of the Guangdong province of China. AmFG and SvFG from sea cucumbers *A. miliaris* and *S. variegatus* were purified as previously reported (Cai et al., 2019). FPA98Cl ion exchange resin was purchased from Rohm and Haas Company (USA). Sephadex G100/G25 and Bio-Gel P10/P6 were obtained from Bio-Rad Laboratories and GE Healthcare company, respectively. Alfa Aesar and aladdin (China) respectively supplied benzethonium chloride and benzyl chloride. Low molecular weight heparin (Enoxaparin, 0.4 mL × 4000 AXaIU) was purchased from Sanofi-Aventis (France). The activated partial thromboplastin time (APTT) reagent, prothrombin time (PT) reagent, thrombin time reagent (TT) reagent, and coagulation control plasma were obtained from Teco Medical (Germany). Biophen FVIII: C kit, Biophen Anti-IIa kits and Biophen Anti-Xa kits were purchased from HYPHEN BioMed (France). Human factor VIII was purchased from Bayer HealthCare LLC (Germany). All other chemicals and reagents were obtained commercially.

2.2. Isolation of HcFG

HcFG was extracted from the sea cucumber *H. coluber* as reported from Yang et al. (2018). The suspension of the body wall was treated by the method of papain enzymolysis and alkaline hydrolysis. The mixture was centrifuged to remove the residue and the supernatant was added with ethanol to a final concentration of 40 % (v/v). After centrifugation, the precipitate was purified by strong ion exchange chromatography using a FPA98 column, eluted sequentially with gradient NaCl solutions. Each elution was dialyzed by ultrafiltration with a 10 kDa molecular weight cut-off membrane (Spectrum Laboratories Inc., USA) and lyophilized. The HcFG fraction mainly eluted with the 2 M NaCl solution. The homogeneity of HcFG was analyzed by the high-performance gel permeation chromatography (HPGPC) (Agilent technologies1260 series apparatus equipped with RID and DAD detectors, Shodex OH pak SB-804 HQ column, 8 mm × 300 mm).

2.3. Depolymerization of HcFG, AmFG and SvFG by β-elimination

As being the mixture of homologues with large molecular weight, it is challenging to elucidate the structure of FG precisely and directly (Zhao et al., 2015). To analyze the fine structure, *β*-elimination depolymerization was employed to HcFG as described previously (Gao et al., 2015). Firstly, HcFG was converted to its quaternary ammonium salt with benzethonium chloride. Secondly, the salt was esterified with benzyl chloride in N, N-Dimethylformamide (DMF). A small amount of the esterification product was taken out to calculate the esterification degree. Then, the rest was depolymerized by 0.08 M EtONa for 0.5 h at room temperature. After precipitation, the intermediate product was reconverted to the sodium salt using saturated sodium chloride solution. Next, the product was treated with NaOH to remove the residual benzyl in aqueous solution, followed by $NaBH_4$ to reduce the hemiacetal groups at the reducing ends in the saccharide chain. Finally, the mixture was neutralized, desalted and lyophilized to yield the depolymerized product dHcFG.

To compare the effects of different FucS branches on the *β*-elimination process, AmFG and SvFG were depolymerized with the same procedure, yielding to dAmFG and dSvFG, respectively.

2.4. Purification of oligosaccharide fractions **H1–H4**

The dHcFG was firstly treated with ultrafiltration membrane (molecular mass cut-off of 10 kDa). Then, the ultrafiltration permeate was separated by gel permeation chromatography (GPC) using Bio-Gel P10 and P6 columns repeatedly. This was monitored by the UV–vis absorption at 232 nm. The eluent in a single peak was collected and desalted, four fractions (**H1–H4**) were ultimately obtained and then analyzed by HPGPC using Superdex peptide 10/300 G L column.

2.5. Molecular weight measurement and NMR analysis

The molecular weight of the native FGs and their *β*-elimination depolymerized products was analyzed by HPGPC (Agilent technologies1260 series apparatus) equipped with RID, DAD detectors (Shodex OH pak SB-804 HQ column, 8 mm × 300 mm), eluted with 0.1 M NaCl at a flow rate of 0.5 mL/min. A standard curve was established using D-series dextran standards (D-1–8, with molecular weight 2,500 Da, 4,600 Da, 7100 Da, 10,000 Da, 21,400 Da, 41,100 Da, 84,400 Da and

133,800 Da), and calibrated by dHSG-2 and dHSG-5 (depolymerized FG with molecular weight 27,800 Da and 5,300 Da). The molecular weight calculation was performed by GPC software (version B01.01, Agilent Co., USA).

NMR experiments were performed at 298 K in D_2O on a 600 or 800 MHz Bruker Avance spectrometer with HOD suppression by pre-saturation. The concentration of the tested samples was 10–20 g/L (Yin et al., 2018).

2.6. Structure optimization of FGs branched with Fuc_{2S4S} and Fuc_{3S4S}

To show the structural details of FGs, the molecular simulation was used in this study. Benzethonium salt of FG was optimized using the Gaussian 09 package (Frisch et al., 2010). Structure optimization and frequency calculation were performed using Density Function Theory (DFT) at B3LYP/sto-3 g level (Hehre, Stewart, & Pople, 1969; Pierotti, 1976).

2.7. Anticoagulation activities and effects on human coagulation factors

APTT, PT, and TT were determined with a coagulometer (TECOMC-4000, Germany) using APTT, PT and TT reagents and standard human plasma as previously described (Shang et al., 2018). Additionally, the iXase inhibitory activity was determined with the reagents in the BIOPHEN FVIII:C Kit (HYPHEN BioMed) according to the previously described method (Buyue & Sheehan, 2009). Anti-thrombin (anti-IIa) and anti-factor Xa (anti-FXa) activities in the presence of AT were measured with Biophen Heparin Anti-IIa kits and Biophen Anti-Xa kits, respectively (Shang et al., 2018).

3. Results and discussion

3.1. Preparation of native HcFG, dHcFG and oligosaccharide fractions

The polysaccharide HcFG was extracted from the sea cucumber *H. coluber* and purified as described previously (Yang et al., 2018). The single symmetric peak in the HPGPC profile (Fig. 1A) indicated the homogeneity of HcFG. Additionally, in its ^{1}H NMR spectrum, the methyl protons at ~1.3 ppm and ~2.0 ppm showed the typical signals from the methyl of Fuc and acetyl group of GalNAc residues in HcFG. The proton signals at region 5.2–5.8 ppm indicated that it possessed several types of FucS (Fig. S1) (Guan et al., 2019; Li et al., 2017). Other physicochemical properties such as molecular weight, IR spectroscopic characteristics and SO_3^-/COO^- molar ratio (3.75:1) were consistent with our previous study (Yang et al., 2018).

As reported before, the structure of HcFG was analyzed preliminarily via the physicochemical properties and its hydrogen peroxide depolymerized product (Yang et al., 2018). However, the exact cleavage position in polysaccharide chain remains unclear and the depolymerized FG was still a mixture of compounds with different molecular weight (Guan et al., 2019).

Selective depolymerization was considered to be a powerful tool to elucidate the precise structures of complex FGs (Cai et al., 2019). To elucidate the fine structure of the native HcFG, its *β*-eliminative depolymerized product was prepared (dHcFG). *β*-Eliminative depolymerization could selectively cleave the β-(1,4) bonds between GalNAc and GlcA residues, and $\Delta^{4,5}$-unsaturated GlcA was formed at the nonreducing termini (Gao et al., 2015).

In this study, dHcFG was dialyzed by ultrafiltration with a 10 kDa molecular mass cut-off membrane to remove the large molecules. The ultrafiltration permeate was further separated by GPC using Bio-Gel P10 and P6 columns repeatedly. Finally, four fractions (**H1–H4**) were obtained and they made up 3.5 %, 10.7 %, 10.3 % and 8.7 % of the HcFG permeate, respectively, according to the peak area calculation by normalization method. The HPGPC profiles (Fig. 1B and C, Superdex peptide 10/300 G L column) showed that the four fractions had a good homogeneity and the retention time were similar with those oligosaccharides that our group reported before. Their structures were clarified by 1D/2D NMR spectroscopy.

3.2. Structural analyses of the oligosaccharide fractions and native HcFG

H1 was proved to be the mixture of trisaccharides. The signals at 5.7–5.8 ppm, formed during the depolymerization process, were

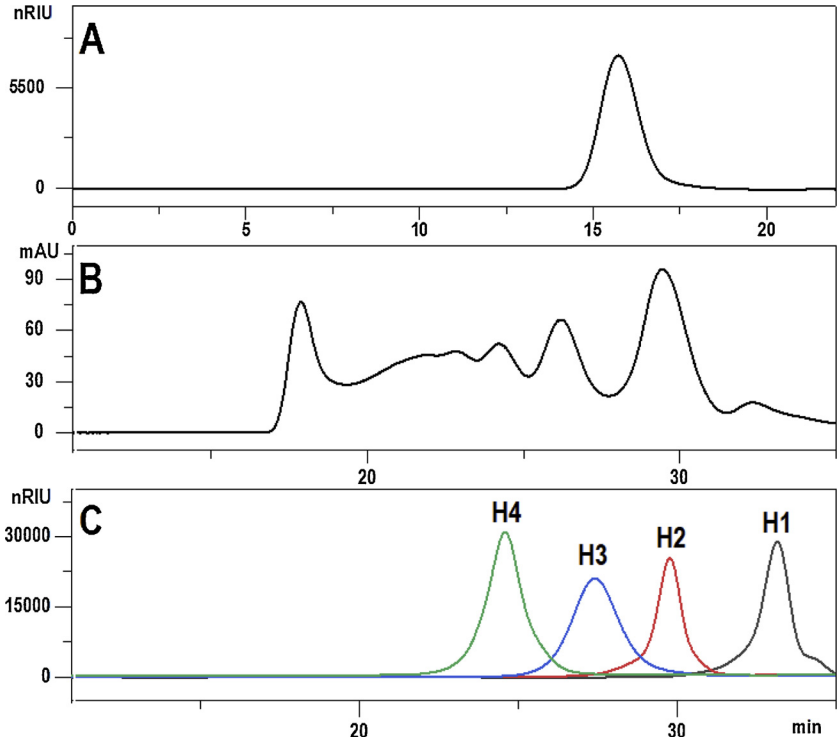

Fig. 1. HPGPC profiles of native HcFG on Shodex OHpak SB-804HQ column eluted with 0.1 M NaCl solution under the differential refractive index detector (RID) (**A**), dHcFG < 10 kDa (**B**) and oligosaccharides (**H1–H4**) (**C**) on Superdex peptide 10/300 G L column eluted with 0.2 M NaCl solution under the diode array detector (DAD) at 232 nm (**B**) and RID (**C**).

assigned to the H-4 of $\Delta^{4,5}$-unsaturated GlcA (dU) branched with different FucS. The signals at 5.42 and 5.21 ppm were ascribed to the anomeric protons of Fuc_{2S4S} and Fuc_{3S4S}, respectively (Fig. S3) (Shang et al., 2018; Yin et al., 2018). Starting with the sets of distinctive peaks, different dU and FucS residues were observed by the ^{1}H-^{1}H COSY and TOCSY spectra (Fig. S3). The sulfation positions of Fuc_{2S4S} and Fuc_{3S4S} were confirmed by the downfield chemical shifts of their H/C-2/4 (4.34/4.62 ppm and 77.6/83.7 ppm) and H/C-3/4 (4.53/4.82 ppm and 78.0/81.7 ppm) (Cai et al., 2019). Similarly, the terminal GalNAc was readily identified by the acetyl group (H/C-8 1.9, 25 ppm; C-7 177 ppm), and amino-functionalized methine (H/C-2 4.2/54 ppm) was linked to a terminal hydroxy-methylene (H/C-1 3.6/62 ppm) that was formed during the $NaBH_4$ reduction post depolymerization. The FucS linked to the O-3 of dU and dU linked to the O-3 of rA were deduced by virtue of the ^{1}H-^{13}C HMBC and ^{1}H-^{1}H ROESY spectra (Fig. S3). A small number of the trisaccharide branched with Fuc_{4S} also existed. The signals were in accordance with those of the trisaccharides derived from the FG from sea cucumber *Holothuria albiventer* (Cai et al., 2019). Additionally, two doublet protons observed at 5.15 and 5.02 ppm were further assigned as the H-1 of Fuc_{2S4S} and Fuc_{3S4S}, while they were attached to the reduced GlcA residues at reducing end, differing from those linked on the dU. The nonreducing end were both GalNAc. The two trisaccharides may be derived from the nonreducing ends of the long chains of the native FG, which were depolymerized and followed by the peeling reaction during the *β*-elimination procedure (Huang et al., 2015). Hence, **H1** was a mixture of trisaccharides with the structures of L-Fuc_{R1}-α1,3-L-$\Delta^{4,5}$GlcA-α1,3-D-$GalNAc_{4S6S}$-ol (R1 was 2,4-di-, 3,4-di- and 4-mono-*O*-sulfation, i.e. 2S4S/3S4S/4S) and L-Fuc_{R2}-α1,3-[D-$GalNAc_{4S6S}$-β1,4-]-D-GlcA-ol (R2 was 2S4S/3S4S) (Figs. 4 and S2).

H2 was determined as a mixture of pentasaccharides. In its ^{1}H NMR spectrum, the signal at 5.67 ppm was the H-4 of dU, while those at 5.0–5.5 ppm were the H-1 of the FucS branches with different types at reducing or nonreducing ends (Fig. 2). Each FucS residue was clearly assigned from the anomeric protons according to the ^{1}H-^{1}H COSY and TOCSY spectra, and their respective sulfation positions were determined by the corresponding downfield chemical shifts. The ^{1}H-^{13}C HMBC and ^{1}H-^{1}H ROESY data indicated that all the FucS residues were linked to the $\Delta^{4,5}$-unsaturated GlcA (dU) at nonreducing end or GlcA-ol (rU) at reducing end existing as mono-fucose (Fig. S5). The integral ratio of the two methyl groups, $-COCH_3$ at ~2.0 ppm from GalNAc and $-CH_3$ at ~1.2 ppm from Fuc, was approximately 1:2, confirmed that **H2** was composed of pentasaccharides containing a GalNAc and two Fuc branched on glucuronic acids (dU and rU). The FucS branches consisted of different patterns of sulfation, including 2S4S/3S4S/4S, with different proportions. Meanwhile, the two sets of proton signals, marked as dI and rI, dII and rII, were identical with two pentasaccharides branched with Fuc_{2S4S} and Fuc_{3S4S} reported previously (Fig. 2) (Cai et al., 2019). Hence, the structure of **H2** was deduced as L-Fuc_{R1}-α1,3-L-$\Delta^{4,5}$GlcA-α1,3-D-$GalNAc_{4S6S}$-β1,4-(L-Fuc_{R2}-α1,3-)-D-GlcA-ol, where R1 represented 2S4S/3S4S/4S and R2 represented 2S4S/3S4S (Fig. 3).

Similarly, after full assignments, on the basis of the structure of **H2**, **H3** was proved to be octa-saccharides with an additional trisaccharide unit -3-D-$GalNAc_{4S6S}$-β1,4-[L-Fuc_{R1}-α1,3]-D-GlcA-β1-. While **H4** was hendeca-saccharides with two additional trisaccharide unit [-3-D-$GalNAc_{4S6S}$-β1,4-(L-Fuc_{R1}-α1,3)-D-GlcA-β1-]$_2$ on the basis of **H2** (Figs. 3 and S6–S9, Tables S3 and S4).

3.3. Structural deduction of the native HcFG

Structural analysis indicated the high regularity of the four fractions **H1–H4** (Fig. 3). Besides L-$Fuc_{2S4S/3S4S}$-α1,3-L-$\Delta^{4,5}$GlcA-α1,3-D-$GalNAc_{4S6S}$-ol in **H1**, all the compounds occurred the peeling reaction, thus losing the GalNAc residues at reducing termini, and then ended as GlcA-ol after reduction with $NaBH_4$. The chain from **H1** to **H4** extended by addition of the trisaccharide unit -3-D-$GalNAc_{4S6S}$-β1,4-(L-Fuc_{R1}-α1,3)-D-GlcA-β1-. Using the "bottom up" strategy, the native HcFG was reassembled to have the general formula of {-β1,4-(L-$Fuc_{2S4S/3S4S/4S}$-α1,3)-D-GlcA-β1,4-D-$GalNAc_{4S6S}$-}$_n$, (n ≈ 58). Its backbone was identical with the chondroitin sulfate E consisting of alternating 4-linked GlcA and 3-linked GalNAc residues within disaccharide repeating units, while all the branches were the mono-fucoses varying with the sulfation patterns. Notably, no Fuc_{3S} branch was found in HcFG. This structure differed from what we characterized before (Yang et al., 2018), indicating that the oxidative depolymerization is inadequate for precise structural characterization, though it could be utilized for structural analysis preliminarily. The hypothetical anomeric proton of Fuc_{3S} may result from the shift of the anomeric proton of FucS locating at different positions in the backbone.

Till now, several native FGs from different sea cucumbers were clearly characterized based on the series of well-defined oligosaccharides. The backbone displayed high uniformity and the main difference was the sulfation types of the fucose branches, single or several ones varying in a species-specific manner (Cai et al., 2019; Guan et al., 2019; Shang et al., 2018; Yin et al., 2018; Zhao et al., 2015).

3.4. Comparative analysis of the depolymerization of AmFG, SvFG and HcFG

The assignments in the ^{1}H NMR spectra of **H2–H4** (Fig. 4) showed that the integral of the anomeric protons of Fuc_{2S4S} at the nonreducing and reducing end (marked as dI_1 and rI_1, respectively) was not equivalent, and those of Fuc_{3S4S} (marked as dII_1 and rII_1, respectively) or Fuc_{4S} were not equivalent as well. This indicated that different FucS branches such as Fuc_{2S4S}, Fuc_{3S4S} or Fuc_{4S} coexisted in the individual oligosaccharide, and in the long chain of the polysaccharide. Interestingly, the integral area of H-1 of Fuc_{2S4S} at the non-reducing end (dI_1, 5.42 ppm) was obviously smaller than that of Fuc_{3S4S} (dII_1, 5.18 ppm) in the ^{1}H NMR spectra of **H2–H4**, implying that the glycoside bonds of β1,4-D-GlcA where the GlcA was branched with Fuc_{3S4S} are inclined to cleave during the *β*-elimination depolymerization.

To find out the difference in different FGs, AmFG, SvFG and HcFG which were branched with Fuc_{3S4S}, Fuc_{2S4S} and several types of FucS (Fuc_{3S4S}, Fuc_{2S4S} and Fuc_{4S}), respectively, were employed to the *β*-elimination depolymerization simultaneously. AmFG, SvFG and HcFG were initially fractionized using Sephadex G100 column to keep the molecular weight as close as possible. Then they were depolymerized by *β*-elimination under the same condition as described in Section 2.3.

Esterification degree is a significant parameter to the depolymerization process. The esterification degrees of the esterification products of AmFG, SvFG and HcFG were 68.4 %, 39.6 % and 48.6 %, respectively, calculated based on the ^{1}H NMR spectra (Fig. S10). The molecular weight of the resulting depolymerized products, dAmFG, dSvFG and dHcFG, were determined by HPGPC (Fig. 5). As shown in Table 1, the molecular weight of AmFG, SvFG and HcFG decreased obviously after depolymerization. The change tendency showed a positive correlation with their esterification degrees. The ratios between the esterification degrees of the FGs approximated to those of the molecular weight between the depolymerized FGs. This would be due to the activation of C-5 proton of GlcA after esterification, which is thus susceptible to cleavage (Kiss, 1974). The results of esterification degree and molecular weight suggested that FG branched with Fuc_{3S4S} was easier to be *β*-elimination depolymerized than that with Fuc_{2S4S}. While the subsequent cleavage by EtONa contributed approximatively to the depolymerization of the FGs regardless of the FucS branches.

3.5. Structure display based on quantum mechanical calculations

To clarify the difference in the esterification degrees between the FGs branched with different sulfation patterns of Fuc, the structures of benzethonium salt of FGs with Fuc_{2S4S} and Fuc_{3S4S} branches were

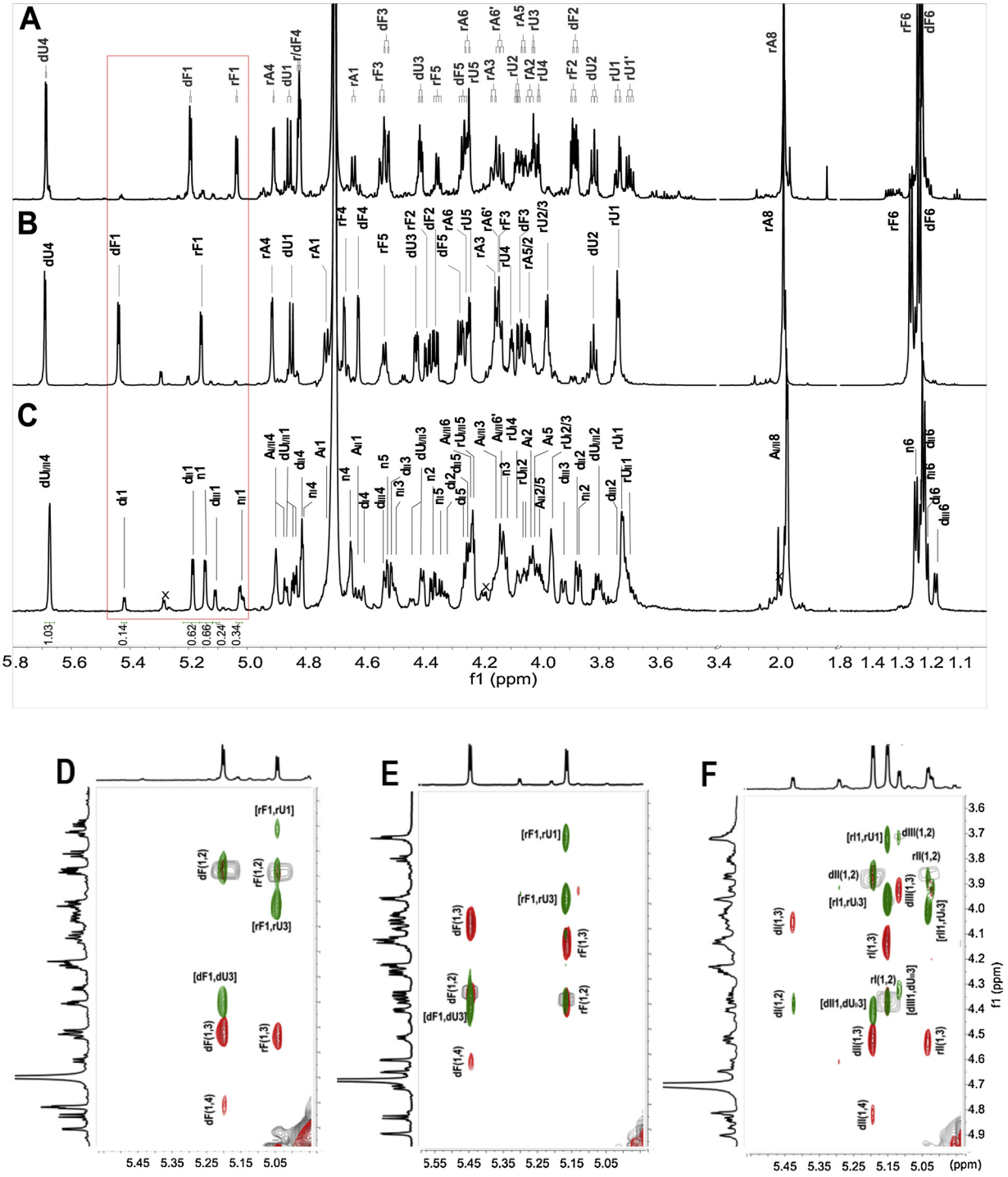

Fig. 2. ^{1}H NMR spectra and signal assignments of pentasaccharides from dAmFG (**A**), dSvFG (**B**) (Cai et al., 2019) and **H2** (**C**), superimposed ^{1}H-^{1}H COSY (black), TOCSY (red) and ROESY (green) spectra of pentasaccharides from dAmFG (**D**), dSvFG (**E**) (Cai et al., 2019) and **H2** (**F**), dI, dII and dIII represent Fuc_{2S4S}, Fuc_{3S4S} and Fuc_{4S} at the nonreducing end, rI and rII represent Fuc_{2S4S} and Fuc_{3S4S} at the reducing termini. (For interpretation of the references to colour in this figure legend, the reader is referred to the web version of this article.)

simulated and optimized based on the Density Function Theory (DFT) at B3LYP/sto-3 g level in DMF as the solvent by the self-consistent reaction field (SCRF) method within a polarizable continuum solvation model (PCM). The final optimized structures have no imaginary frequencies, indicating that the structure corresponds to a local minimum on the potential energy surface.

As shown in Fig. 6, FGs branched with different FucS produce quaternary ammonium salts with significant differences in structure. In the optimized structure of benzethonium salt of FG with Fuc_{2S4S} branches, the benzene ring is close to the carboxyl group of the GlcA in the backbone, which was the esterified position during the β-elimination depolymerization, resulting in steric hindrance effect (Fig. 6A). While in that of the FG with Fuc_{3S4S} branches, little steric effect at the same position was found (Fig. 6B). This result may provide some clues to explain the differences in the esterification degrees reasonably.

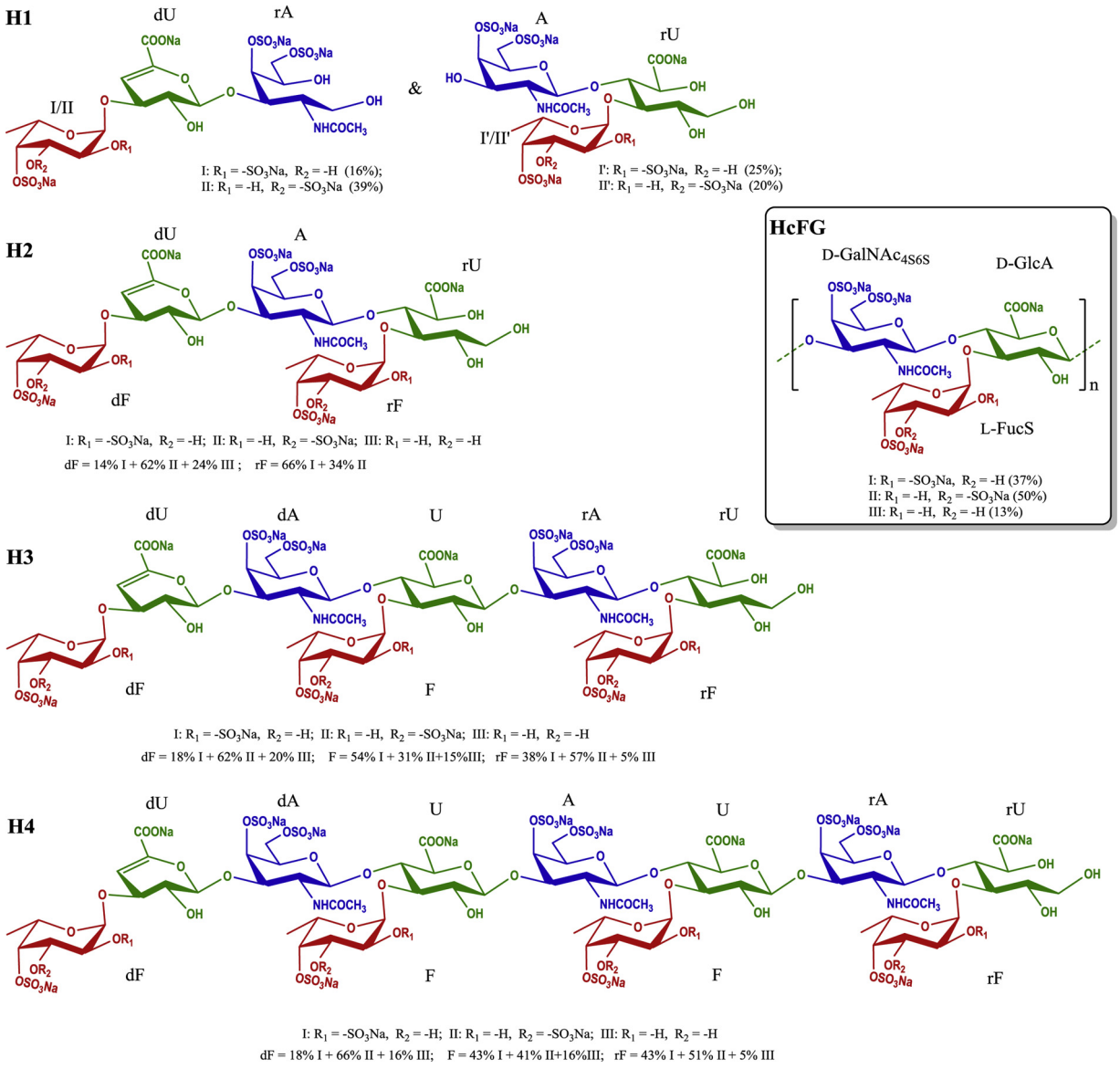

Fig. 3. Structures of **H1–H4** and the native HcFG.

3.6. Anticoagulant activity and effects on coagulation factors

Herein, the anticoagulant activities of the three native FGs containing different sulfation types of FucS branches, AmFG, SvFG, HcFG, and their *β*-eliminative depolymerized derivatives, dAmFG, dSvFG and dHcFG, were assessed by measuring the APTT, PT and TT of normal human plasma, compared with the positive control LMWH (Table 1). The assays showed that all the samples exhibited significant APTT prolonging activity. The concentrations required to double APTT were in the range of 3–6 μg/mL, while that of LMWH was 14.4 μg/mL. Overall, the depolymerized products showed slightly weaker activity than the native FGs with the decrease in molecular weight. Additionally, the three native FGs displayed obvious TT prolonging activity in the range of 7–13 μg/mL, while this activity markedly declined after depolymerization. All the samples exhibited no obvious effect on PT at the concentration as high as 128 μg/mL. These results indicated that the FGs and its derivatives mainly affected the intrinsic coagulation pathway while they had little effect on the extrinsic coagulation pathway. Besides, the native FGs also had certain effect on the common coagulation pathway.

Furthermore, the effects of these samples on coagulation factors and cofactors were evaluated. As shown in Table 1 and Fig. S11, all the native and depolymerized FGs potently inhibited the iXase, though the molecular weight significantly decreased after depolymerization. And the iXase inhibitory activity was much stronger than the AT-dependent IIa and Xa inhibitory activities. Meanwhile, the negligible difference in the iXase inhibitory activity of the native and depolymerized FGs branched with different FucS types suggested that the FucS patterns affected the potency of the anti-iXase activity slightly when the molecular weight was up to a certain degree.

Additionally, the activities of four oligosaccharides **H1–H4** obtained from dHcFG were also evaluated. Compared with the native FGs and depolymerization products, APTT prolonging effects of the oligosaccharides were much weaker and they had no effects on PT and TT. The anticoagulant effects of **H3** and **H4** had a good correlation with their anti-iXase activities. The potent iXase inhibitory activity was still retained while the AT-dependent IIa inhibitory activity declined rapidly. The results further confirmed that the selectivity of the iXase inhibition of the depolymerized FG has increased. The maintenance of anticoagulant effect might require a certain chain length and octasaccharide is the minimum fragment for such potent activity (Cai et al., 2019; Yin et al., 2018).

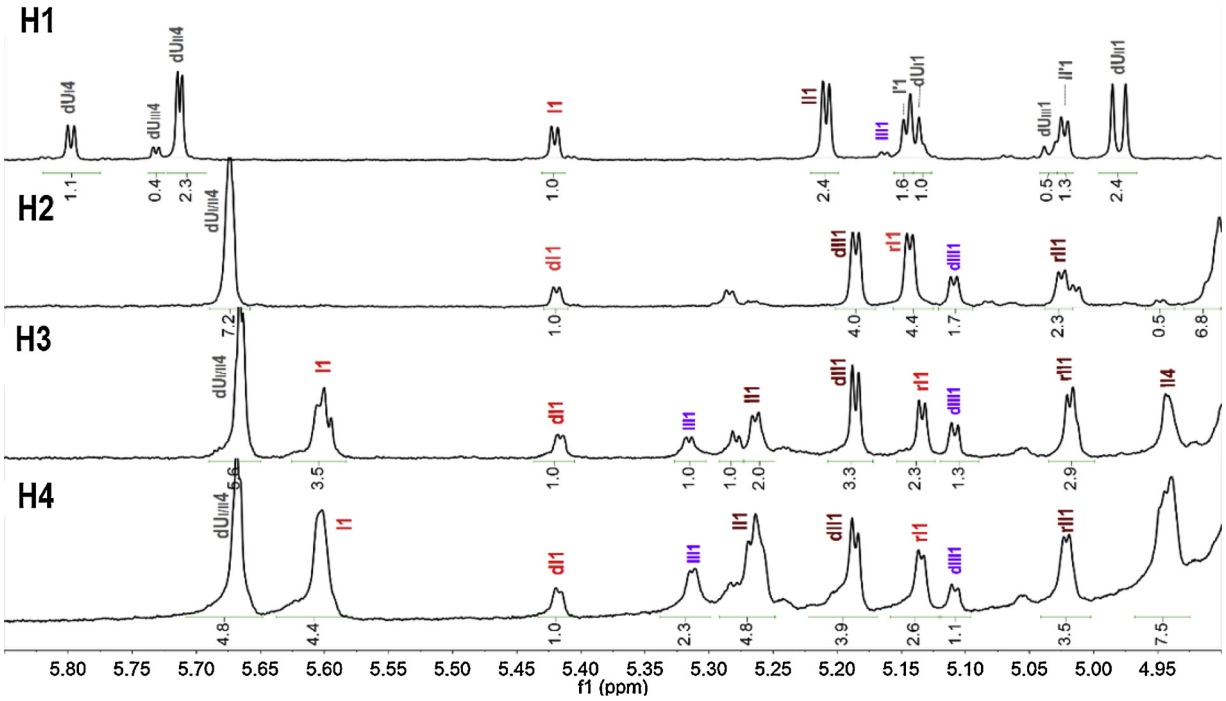

Fig. 4. Proton signals comparison at the downfield region (4.80–5.90 ppm) of **H1** – **H4**.

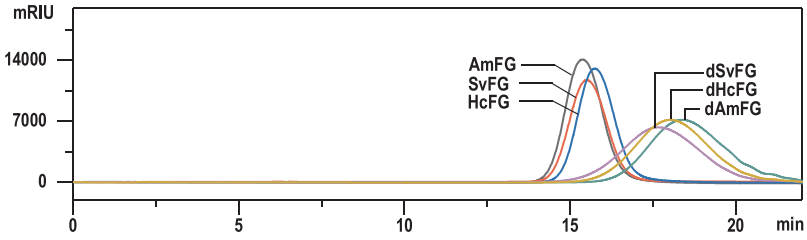

Fig. 5. HPGPC profiles of the fractionized AmFG, SvFG, HcFG and their depolymerized products dAmFG, dSvFG, dHcFG (Shodex OHpak SB-804HQ column, 0.1 M NaCl solution, RID).

Table 1
The molecular weights and anticoagulant properties of AmFG, SvFG HcFG and the depolymerized products.

	FucS branch type	Mw (kDa)	Mn	Mw/Mn	APTT[a] (μg/mL)	TT[a]	anti-iXase[b] IC_{50} (ng/mL)	anti-IIa (AT)[b]	anti-Xa (AT)[b]
AmFG	II	67.5	60.4	1.12	3.32	12.5	28.3 ± 0.8	2010 ± 439	> 10,000
SvFG	I	63.3	57.7	1.10	3.87	7.90	40.5 ± 1.3	411 ± 15	3630 ± 58
HcFG	I/II/III	54.9	50.0	1.10	3.31	7.68	26.4 ± 1.0	1260 ± 169	> 10,000
dAmFG	II	6.20	4.54	1.37	6.15	> 128	16.7 ± 0.4	2970 ± 954	> 10,000
dSvFG	I	9.77	6.83	1.43	4.48	> 128	20.8 ± 0.6	1660 ± 37	> 10,000
dHcFG	I/II/III	7.93	5.73	1.38	5.30	> 128	23.5 ± 2.1	1970 ± 171	> 10,000
H4	I/II/III	3.42	/[c]	/	18.7	> 128	137 ± 10	> 10,000	> 10,000
H3	I/II/III	2.46	/	/	47.9	> 128	703 ± 59	> 10,000	> 10,000
H2	I/II/III	1.56	/	/	> 128	> 128	> 10,000	> 10,000	> 10,000
H1	I/II/III	0.96	/	/	> 128	> 128	> 10,000	> 10,000	> 10,000
LMWH		4.50	/	/	14.4	3.16	152 ± 10	50.8 ± 3.0	46.9 ± 2.0

[a] Concentration required to double the APTT/PT of human plasma.
[b] IC_{50} value, concentration required to inhibit 50 % of protease activity.
[c] No data.

4. Conclusion

In this work, the precise structure of FG extracted from the sea cucumber *H. coluber* was clearly deduced as {-β1,4-(L-FucS-α1,3-)-D-GlcA-β1,4-D-$GalNAc_{4S6S}$-}$_n$ based on the well-defined oligosaccharide fractions **H1**–**H4**, where FucS was Fuc_{2S4S}, Fuc_{3S4S} and Fuc_{4S} with the ratio of 37 %:50 %:13 %. Till now, all the proven FGs deduced from their purified fragments displayed the high regularity that the backbone of FG was identical with that of chondroitin sulfate E, a common GAG ubiquitously distributed in mammal, and all the branches were mono-fucose linked to the O-3 of GlcA in the backbone. While the FucS branches were sulfated at different positions in different proportions, varying from the sea cucumber species.

The structures of the penta-, octa-, hendeca-saccharides (**H2–H4**) showed that different FucS branches could coexist in the same chain of FG. Different susceptibilities to *β*-eliminative depolymerization was observed and the GlcA branched with Fuc_{3S4S} were more prone to cleavage than that branched with Fuc_{2S4S}. This may be due to the different steric hindrance effects from the FucS on the esterification of GlcA. The simulation result showed the possibility of steric hindrance as

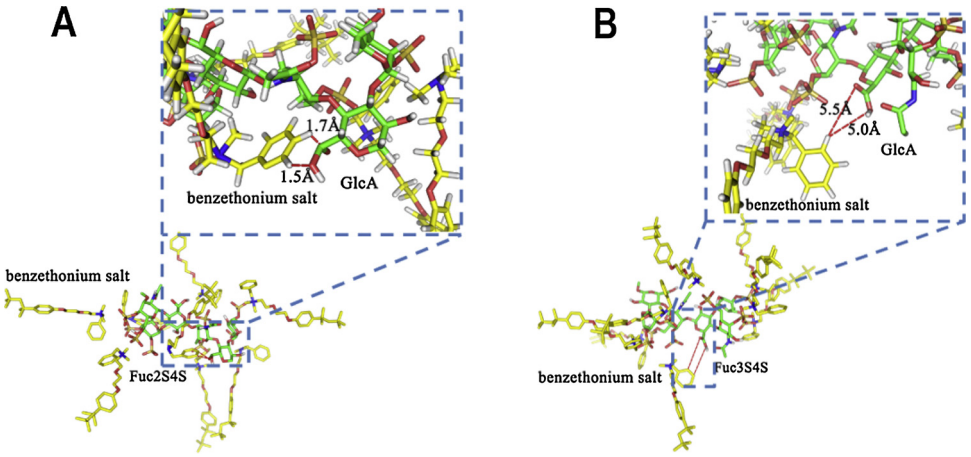

Fig. 6. The structures of benzethonium salt of FGs branched with Fuc_{2S4S} (A) and with Fuc_{3S4S} (B). The benzethonium salt is marked in yellow, and FG is marked in green. (For interpretation of the references to colour in this figure legend, the reader is referred to the web version of this article.)

well.

Biological assays indicated that the native and depolymerized FGs exhibited potent anticoagulant activity by inhibiting iXase and the target selectivity of the anticoagulant activity has increased after depolymerization. Structure and activity relationship analysis showed that the different FucS patterns had almost no affect on the anti-iXase activity when the chain length was long enough. The octasaccharide was the minimum fragment retaining the potent iXase inhibitory activity.

Acknowledgments

This work was funded in part by the National Natural Science Foundation of China (81773737, 81703374, 81872774, 81673330 and 31900926) and the Yunnan Innovative Research Team (2018HC012).

Appendix A. Supplementary data

Supplementary material related to this article can be found, in the online version, at doi:https://doi.org/10.1016/j.carbpol.2020.115844.

References

Bordbar, S., Anwar, F., & Saari, N. (2011). High-value components and bioactives from sea cucumbers for functional foods–a review. *Marine Drugs, 9*(10), 1761–1805.

Borsig, L., Wang, L., Cavalcante, M. C. M., Cardilo-Reis, L., Ferreira, P. L., Mourão, P. A., et al. (2007). Selectin blocking activity of a fucosylated chondroitin sulfate glycosaminoglycan from sea cucumber. Effect on tumor metastasis and neutrophil recruitment. *The Journal of Biological Chemistry, 282*(20), 14984–14991.

Buyue, Y., & Sheehan, J. P. (2009). Fucosylated chondroitin sulfate inhibits plasma thrombin generation via targeting of the factor IXa heparin-binding exosite. *Blood, 114*(14), 3092–3100.

Cai, Y., Yang, W., Li, X., Zhou, L., Wang, Z., Lin, L., et al. (2019). Precise structures and anti-intrinsic tenase complex activity of three fucosylated glycosaminoglycans and their fragments. *Carbohydrate Polymers, 224*, 115146.

Fonseca, R. J., Santos, G. R., & Mourão, P. A. (2009). Effects of polysaccharides enriched in 2,4-disulfated fucose units on coagulation, thrombosis and bleeding. *Thrombosis and Haemostasis, 102*(5), 829–836.

Frisch, M. J., Trucks, G. W., Schlegel, H. B., Scueria, G. E., Robb, M. A., Cheeseman, J. R., et al. (2010). *Gaussian 09 revision C.01*. Wallingford, CT: Gaussian Inc.

Gao, N., Lu, F., Xiao, C., Yang, L., Chen, J., Zhou, K., et al. (2015). β-Eliminative depolymerization of the fucosylated chondroitin sulfate and anticoagulant activities of resulting fragments. *Carbohydrate Polymers, 127*, 427–437.

Guan, R., Peng, Y., Zhou, L., Zheng, W., Liu, X., Wang, P., et al. (2019). Precise structure and anticoagulant activity of fucosylated glycosaminoglycan from *Apostichopus japonicus*: Analysis of its depolymerized fragments. *Marine Drugs, 17*, 195.

Hehre, W. J., Stewart, R. F., & Pople, J. A. (1969). Self-consistent molecular orbital methods. 1.Use of Gaussian expansions of Slater-type atomic orbitals. *The Journal of Chemical Physics, 51*, 2657–2664.

Huang, Y., Mao, Y., Zong, C., Lin, C., Boons, G. J., & Zaia, J. (2015). Discovery of a heparan sulfate 3-O-sulfation specific peeling reaction. *Analytical Chemistry, 87*(1), 592–600.

Kariya, Y., Watabe, S., Kyogashima, M., Ishihara, M., & Ishii, T. (1997). Structure of fucose branches in the glycosaminoglycan from the body wall of the sea cucumber *Stichopus japonicus*. *Carbohydrate Research, 297*(3), 273–279.

Kitazato, K., Kitazato, K. T., Nagase, H., & Minamiguchi, K. (1996). DHG, a new depolymerized holothurian glycosaminoglycan, exerts an antithrombotic effect with less bleeding than unfractionated or low molecular weight heparin, in rats. *Thrombosis Research, 84*(2), 111–120.

Kariya, Y., Watabe, S., Hashimoto, K., & Yoshida, K. (1990). Occurrence of chondroitin sulfate E in glycosaminoglycan isolated from the body wall of sea cucumber *Stichopus juponicus*. *The Journal of Biological Chemistry, 265*(9), 5081–5085.

Kiss, I. (1974). β-Eliminative degradation of carbohydrates containing uronic acid residues. *Advances in Carbohydrate Chemistry and Biochemistry, 29*(8), 229–303.

Li, J., & Lian, E. (1988). Aggregation of human platelets by acidic mucopolysaccharide extracted from *Stichopus japonicus* Selenka. *Thrombosis and Haemostasis, 59*(3), 435–439.

Li, X., Luo, L., Cai, Y., Yang, W., Lin, L., Li, Z., et al. (2017). Structural elucidation and biological activity of a highly regular fucosylated glycosaminoglycan from the edible sea cucumber *Stichopus herrmanni*. *Journal of Agricultural and Food Chemistry, 65*, 9315–9323.

Mou, J., Li, Q., Qi, X., & Yang, J. (2018). Structural comparison, antioxidant and anti-inflammatory properties of fucosylated chondroitin sulfate of three edible sea cucumbers. *Carbohydrate Polymers, 185*, 41–47.

Myron, P., Siddiquee, S., & Al Azad, S. (2014). Fucosylated chondroitin sulfate diversity in sea cucumbers: A review. *Carbohydrate Polymers, 112*, 173–178.

Pierotti, R. A. (1976). A scaled particle theory of aqueous and nonaqueous solutions. *Chemical Reviews, 76*(6), 717–726.

Pomin, V. H. (2014). Holothurian fucosylated chondroitin sulfate. *Marine Drugs, 12*(1), 232–254.

Santos, G. R., Porto, A. C., Soares, P. A., Vilanova, E., & Mourão, P. A. (2017). Exploring the structure of fucosylated chondroitin sulfate through bottom-up nuclear magnetic resonance and electrospray ionization-high-resolution mass spectrometry approaches. *Glycobiology, 27*(7), 625–634.

Shang, F., Gao, N., Yin, R., Lin, L., Xiao, C., Zhou, L., et al. (2018). Precise structures of fucosylated glycosaminoglycan and its oligosaccharides as novel intrinsic factor Xase inhibitors. *European Journal of Medicinal Chemistry, 148*, 423–435.

Sheehan, J. P., & Walke, E. N. (2006). Depolymerized holothurian glycosaminoglycan and heparin inhibit the intrinsic tenase complex by a common antithrombin-independent mechanism. *Blood, 107*(10), 3876–3882.

Ustyuzhanina, N. E., Bilan, M. I., Dmitrenok, A. S., Tsvetkova, E. A., Shashkov, A. S., Stonik, V. A., et al. (2016). Structural characterization of fucosylated chondroitin sulfates from sea cucumbers *Apostichopus japonicus* and *Actinopyga mauritiana*. *Carbohydrate Polymers, 153*, 399–405.

Ustyuzhanina, N. E., Bilan, M. I., Nifantiev, N. E., & Usov, A. I. (2019). Structural analysis of holothurian fucosylated chondroitin sulfates: Degradation versus non-destructive approach. *Carbohydrate Research, 476*, 8–11.

Vieira, R. P., Mulloy, B., & Mourão, P. A. (1991). Structure of a fucose-branched chondroitin sulfate from sea cucumber. Evidence for the presence of 3-O-sulfo-beta-D-glucuronosyl residues. *The Journal of Biological Chemistry, 266*(21), 13530–13536.

Vieira, R. P., & Mourão, P. A. (1988). Occurrence of a unique fucose-branched chondroitin sulfate in the body wall of a sea cucumber. *The Journal of Biological Chemistry, 263*(34), 18176–18183.

Wu, M., Wen, D., Gao, N., Xiao, C., Yang, L., Xu, L., et al. (2015). Anticoagulant and antithrombotic evaluation of native fucosylated chondroitin sulfates and their derivatives as selective inhibitors of intrinsic factor Xase. *European Journal of Medicinal Chemistry, 92*, 257–269.

Yan, L., Li, J., Wang, D., Ding, T., Hu, Y., Ye, X., et al. (2017). Molecular size is important for the safety and selective inhibition of intrinsic factor Xase for fucosylated chondroitin sulfate. *Carbohydrate Polymers, 178*, 180–189.

Yang, J., Wang, Y., Jiang, T., & Lv, Z. (2015). Novel branch patterns and anticoagulant activity of glycosaminoglycan from sea cucumber *Apostichopus japonicus*. *International Journal of Biological Macromolecules, 72*, 911–918.

Yang, W., Cai, Y., Yin, R., Lin, L., Li, Z., Wu, M., et al. (2018). Structural analysis and anticoagulant activities of two sulfated polysaccharides from the sea cucumber *Holothuria coluber*. *International Journal of Biological Macromolecules, 115*, 1055–1062.

Yin, R., Zhou, L., Gao, N., Li, Z., Zhao, L., Shang, F., et al. (2018). Oligosaccharides from depolymerized fucosylated glycosaminoglycan: Structures and minimum size for intrinsic factor Xase complex inhibition. *The Journal of Biological Chemistry, 293*(36), 14089–14099.

Yoshida, K., & Minami, Y. (1992). Structure of DHG, a depolymerized holothurian glycosaminoglycan from sea cucumbe. *Tetrahedron Letters, 33*(34), 4959–4962.

Zhao, L., Lai, S., Huang, R., Wu, M., Gao, N., Xu, L., et al. (2013). Structure and anticoagulant activity of fucosylated glycosaminoglycan degraded by deaminative cleavage. *Carbohydrate Polymers, 98*(2), 1514–1523.

Zhao, L., Wu, M., Xiao, C., Yang, L., Zhou, L., Gao, N., et al. (2015). Discovery of an intrinsic tenase complex inhibitor: Pure nonasaccharide from fucosylated glycosaminoglycan. *Proceedings of the National Academy of Sciences of the United States of America, 112*(27), 8284.